Dalton Transactions

Accepted Manuscript

This article can be cited before page numbers have been issued, to do this please use: B. N. Mongal, A. Tiwari, C. Malapaka and U. Pal, *Dalton Trans.*, 2019, DOI: 10.1039/C9DT01506J.

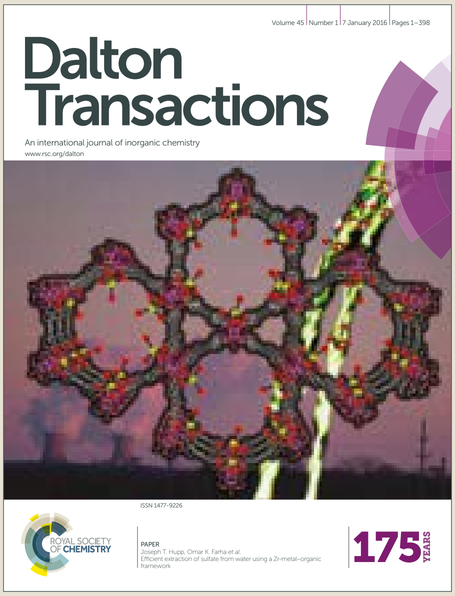

TOC

View Article Online
DOI: 10.1039/C9DT01506J

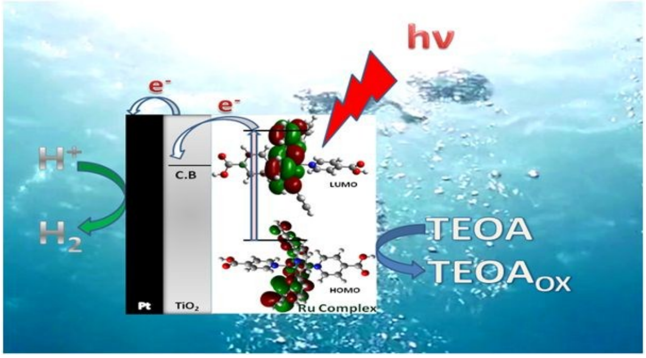

Bis-(hydroxyphenyl) bipyridine based ruthenium complexes as photosensitizers for efficient photocatalytic H_2 evolution.

Ruthenium(III)-bis(phenolato)bipyridine/TiO_2 hybrids: unprecedented photocatalytic hydrogen evolution

View Article Online
DOI: 10.1039/C9DT01506J

Received 00th January 20xx,
Accepted 00th January 20xx

DOI: 10.1039/x0xx00000x

www.rsc.org/

Binitendra Naath Mongal,[*†,#] Amritanjali Tiwari, [‡,§] Malapaka Chandrasekharam, [†,§] and Ujjwal Pal[*‡,§]

Abstract

In this work, two new bis-(hydroxyphenyl)bipyridine based ruthenium complexes with 4-picoline (coded as MCS-B4M) and isonicotinic acid (coded as MCS-B5M) as ancillary ligands have been synthesized and employed for the first time as photosensitizers in photocatalytic hydrogen evolution studies. The photocatalyst MCS-B5M/TiO_2-Pt showed impressive hydrogen generation rate, up to 4.2 mmolh-1 and turn over number (TON) of 84,959 after 5h has been achieved. The better performance of B5TP over B4TP is due to the higher excited state lifetime of MCS-B5M (~ 2.6 ns) over MCS-B4M (~1.4 ns) leads to higher probability of electron transfer to TiO_2/Pt composite in case of the former and stronger coupling of MCS-B5M excited states with the conduction band of the TiO_2/Pt composite by the –COOH linkers of isonicotinic acid moiety results in better photosensitization as observed in UV-Vis (DRS mode) absorbance study The comparative study of the two dyes clearly shows the manifestations of their respective ancillary ligands having contrasting electronic properties. This work gives a new class of ruthenium photosensitizers as efficient light harvesting photocatalyst.

Introduction

Splitting water into hydrogen and oxygen with sunlight is an attractive sustainable energy conversion idea compatible with the concept of energy democracy.[1] Efficient photophysical processes combined with catalyst driven transformations are highly warranted to achieve this thermodynamically uphill reaction.[2-4]Sensitising a wide band-gap semiconductor with a redox photosensitizer to produce H_2 has been an effective way of solar-to-fuel conversion. Widely employed photosensitizers for this application include polypyridyl complexes of ruthenium,[5-8] platinum,[9,10] iridium,[11,12] organic chromophores,[13-16] perovskites[17] and molecular dyads.[18] Recently, our group reported efficient photocatalytic hydrogen evolution using novel thiocyanate based ruthenium dyes.[19] In continuation of our efforts, we report here, the synthesis of two bis-(hydroxyphenyl)bipyridine based ruthenium complexes (coded as MCS-B4M and MCS-B5M) (Figure 1) and studied their TiO_2-Pt composites (coded B4TP and B5TP respectively) for photocatalytic H_2 production wherein the reductive half-reaction of H_2 generation from aqueous protons under visible light irradiation has been discussed. Scheme 1 depicts the synthetic outline for the preparation of both the complexes. While our work was in progress, a ruthenium complex similar to MCS-B4M with a hexafluorophosphate counter-anion has been reported by Lau et al. where CAN driven oxidative degradation of the complex has been studied.[20] To the best of our knowledge, this is the first time when ruthenium complexes of 6,6'-(bis-phenolato)bypyridine ligand have been employed as photosensitizers for efficient photocatalytic H_2 production under visible light region of the solar spectrum.

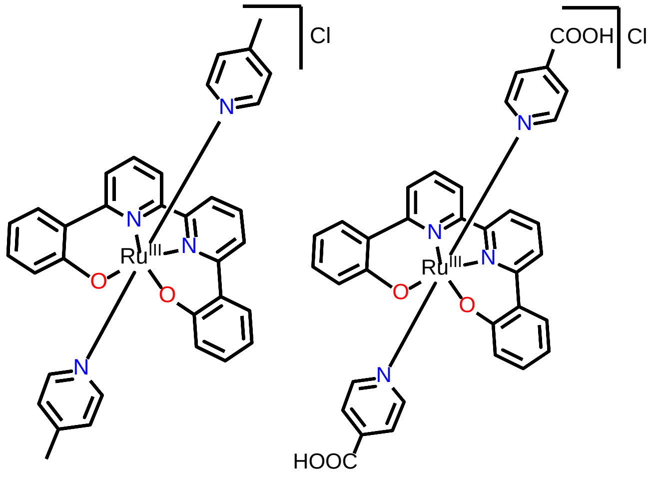

Fig. 1. Structural representation of **MCS-B4M** (left) and **MCS-B5M** (right).

[†]Polymer & Functional Materials Division, CSIR-Indian Institute of Chemical Technology, Hyderabad, India
[‡]Centre for Environmental Engineering and Fossil Fuels, CSIR-Indian Institute of Chemical Technology, Hyderabad, India
[§]Academy of Scientific and Innovative Research (AcSIR), New Delhi, India

Electronic Supplementary Information (ESI) available: The supporting information is available free of charge in the ACS website. Additional information including structural characterization like ^1H-NMR, ESI-MS, HRMS and DFT optimized parameters.

[#]Currently in School of Basic and Applied Sciences, GD Goenka University, Gurgaon, India

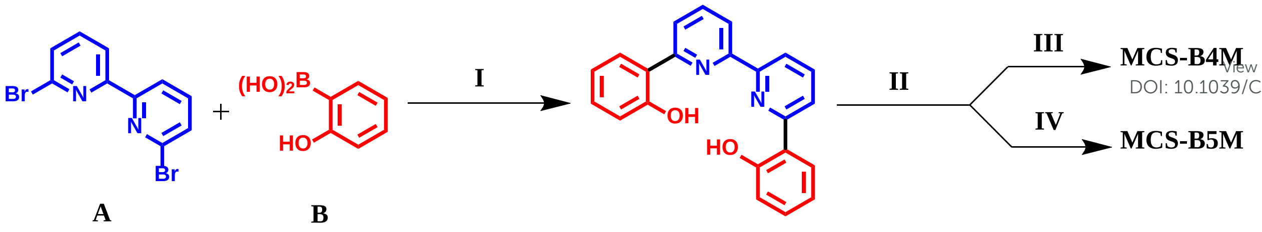

A: 6,6-dibromo-2,2-bipyridine
B: 2-hydroxybenzene boronic acid

Reaction conditions: I. $Pd(PPh_3)_4$, Na_2CO_3, DME:H_2O(4:1); II. $Ru(DMSO)_4Cl_2$, EtOH, 80 °C, reflux, 24 hrs; III. 4-Picoline, EtOH, 80 °C, reflux, 12 hrs IV. Isonicotinic acid, EtOH, 80 °C, reflux, 12 hrs

Scheme 1. Synthetic route of the metal complexes

Experimental

Materials and Methods

6,6'-dibromo-2,2'-bipyridine was purchased from TCI chemicals. 2-hydroxybenzene boronic acid was purchased from alfa aesar. $Ru(DMSO)_4Cl_2$ was prepared from $RuCl_3$ according to the reported procedure. 4-Picoline and isonicotinic acid were purchased from sigma Aldrich. Ethanol and DMSO used were HPLC grade. Water used for the spectrophotometric and electrochemical studies was purified by a Milli-Q system. Tetrabutyl ammonium perchlorate was synthesized according to literature.[21] UV–Vis spectra in absorbance and DRS mode were recorded using a Shimadzu UV-3600 spectrophotometer. The pH values were measured in a Thermos Scientific Orion 4 star pH Benchtop. Photoluminescence experiments measured in JASCO FP-8300 spectrofluorometer. Time-resolved fluorescence measurements have been carried out using HORIBA Jobin Yvon spectrofluorometer. The count rates employed were typically $10^3 – 10^4$ s^{-1}. Deconvolution of the data was carried out by the method of iterative reconvolution of the instrument response function and the assumed decay function using DAS-6 software. The goodness of the fit of the experimental data to the assumed decay function was judged by the standard statistical tests (i.e., random distribution of weighted residuals, the autocorrelation function and the values of reduced χ^2). Infrared spectra were recorded as KBr pellets on a Shimadzu IR-Prestige21 spectrometer. A Conventional three electrode assembly was used under nitrogen to record cyclic voltammograms in CHI6003E potentiostat. The working electrode was glassy carbon. The counter electrode was a platinum wire and Ag/AgCl was used as the reference electrode. The scan rate was 5 mV/s. The 0.10 M anhydrous tetrabutylammonium perchlorate (TBAP) solution in the acetonitrile was used as a supporting electrolyte. The 1 mM solutions of each compound were used for measurement. The ferrocene/ferrocenium couple was observed at E^0 (ΔEp) = 0.4 V (5 mV) under these experimental conditions. ^1H NMR spectra were recorded on a Bruker AVANCE DPX 400 MHz spectrometer using $Si(CH_3)_4$ as internal standard. ESI-MS and HRMS of the samples were recorded on Thermofischer orbitrap. EPR spectrum was recorded in JEOL: JES-FA200.

Theoretical Calculation

All theoretical calculations were carried out using the density functional theory (DFT) approach with a suite in Gaussian 09 programs.[22] Ground state geometries are optimized in the gas phase with the RPBE1PBE functional with def2-SVP with effective-core potential (ECP) was used for Ru and for the rest of the elements def2-SVP was used.[23]

Synthesis

Preparation of ligands

6,6'-bis(2-hydroxyphenyl)-2,2'-bipyridine(LH2): The 6,6-dibromo-2,2-bipyridine (0.1 g, 0.32 mmol), 2-hydroxybenzene boronic acid (0.88 g, 0.64 mmol) and Na_2CO_3 (4.48 g, 14 mmol) were dissolved in 20 mL of in DME/H_2O (4:1, v/v, 20mL). The $Pd(PPh_3)_4$ (5 mol%) was added as a catalyst. The mixture was stirred at 90°C under N_2 for 24 h. The organic layers, extracted with CH_2Cl_2 and dried with anhydrous Na_2SO_4. The crude product was purified by column chromatography (Hexane:EtOAc 80:20, v/v) to obtain a light yellow coloured solid.(65 mg, 60%). Mass: 341$(M+H)^+$ ^1H-NMR ($CDCl_3\delta$): 14.2(2H,s,NH), 8.15(2H,d,H_i), 8.04(4H,m,$H_{d,h}$), 7.85(2H,d,H_g), 7.35(2H,t,H_b), 7.1(2H,d,H_a), 6.98(2H,t,H_c).

Preparation of Complexes

[Ru(III)(L)(4-picoline)$_2$]Cl (MCS-B4M): The ligand LH_2 (100 mg, 0.29 mmol)) was dissolved in 10 ml EtOH in a round bottom flask. The solution was slowly heated with drop wise addition of 0.5 mL Et_3N and then $Ru(DMSO)_4Cl_2$ was added and the reaction mixture was refluxed for 24 hours under N_2 atmosphere. Excess 4-picoline was directly added into the reaction mixture and refluxed further for 12 hours. The crude product was extracted with DCM and purified with DCM:MeOH (99:1) to give a dark green coloured solid (20 mg). Mass: 626$(M+H)^+$ High Resolution Mass Spectrum: 626.12551 (calcd. 626.12503). Elemental analysis calculated for $C_{34}H_{28}N_4O_2Ru$: % C 65.27, H 4.51, N 8.95; Found %: C 65.38, H 4.76, N 8.88. Selected IR bands (cm^{-1}): 3304 ($\nu_{C–H}$), 1650 ($\nu_{C=C}$), 1386 (ν_{C-O}).

[Ru(III)(L)(Isonicotinic acid)$_2$]Cl (MCS-B5M): The synthesis procedure is same as that of the above complex with excess isonicotinic acid in place of 4-picoline. After completion of the reaction, the solvent is reduced to 1 mL and the product is

View Article Online
DOI: 10.1039/C9DT01506J

precipitated with addition of water. The dark green coloured crude product is purified with DCM:MeOH (90:10) to give a dark green coloured solid (30 mg). Mass: 686 $(M+H)^+$ High Resolution Mass Spectrum: 686.07715 (calcd. 686.07339). Elemental analysis calculated for $C_{34}H_{24}N_4O_6Ru$: % C 59.56, H 3.53, N 8.17; Found %: C 59.63, H3.83, N 8.58. Selected IR bands (cm^{-1}): 3290 ($\nu_{O–H}$), 2921(ν_{C-H}), 1644 ($\nu_{C=O\ symm.}$), 1463($\nu_{C=C}$), 1382 ($\nu_{C=O\ assym.}$).

Deposition of Pt on TiO_2 composite

To improve the better photocatalytic activity of H_2 production, 1 wt % Pt metal was deposited onto the surface of the catalysts by using the previously reported method[15]. In 100 ml glass reaction vessel, 1.0 g of each catalyst was dispersed in 30 ml methanol. Then, aqueous solution of H_2PtCl_6 (0.25 ml, 8 wt % aqueous solution) was added into the methanolic suspension of TiO_2 and reaction mixture was irradiated by a 450 W Hg lamp for 45 minutes. The resultant Pt-TiO_2 composite of light gray colour was retrieved by centrifugation, washed three times with excess methanol and dried under vacuum at 70^o C. Pt deposition is confirmed by TEM analysis (see Figure S8 in ESI).

Dye adsorption on Pt-TiO_2

To develop the visible light-driven catalytic systems for water splitting, Pt nanoparticles were loaded on commercial TiO_2 nanoparticles by a known method.[24] Then, the prepared sensitizers were adsorbed on TiO_2-Pt composites by treating with acetonitrile-ethanol solution (1:1 v/v, 20 mL) of the 0.5 µmol concentration of dyes. After retrieving the sensitizer-TiO_2-Pt composites by centrifugation, the remaining solution became colourless, indicating that the dyes were completely adsorbed on TiO_2-Pt nanoparticles. The FTIR spectra of the composites have been measured to ascertain the binding modes of the dyes with TiO_2 (Fig. S10).

FTIR: **B4TP** (cm^{-1}): 2971, 2932, 2150, 1843, 1602, 1559, 1459, 1317, 1261.

B5TP (cm^{-1}): 2923, 2858, 1719, 1597, 1555, 1459, 1420, 1308, 1269.

Photocatalytic Experiments

Photocatalytic H_2 generation experiments were carried out in a doubly jacketed Pyrex glass reactor with flat optical window and external cooling jacket. All experiments were carried over 20 mL aqueous suspension of 15 mg photocatalyst containing 10 vol % of TEOA as sacrificial electron donor (SED). The solution was adjusted to the desired pH using 1 M hydrochloric acid. It was then air sealed with a rubber septum. Before light irradiation dissolved air was removed by 20 min high vacuum followed by purging of Ar gas. An Oriel Instruments solar simulator equipped with a 300 W xenon arc lamp system with cutoff filter ($\lambda \geq 420$ nm) as irradiation source was employed. Above filter can be easily replaced with any other wavelength cutoff filter to alter the radiation wavelength regime. Reaction vessel was kept 20 cm away from the light source to ensure the one sun condition, as suggested by Oriel solar 85 simulator manual. Gas analysis was carried out by regular sampling after every hour, and a gas chromatograph (GC) equipped with TCD detector 90 (Agilent 7890) was employed for quantitative analysis.

Results and discussion

Synthetic procedure

The ligand LH2 was prepared by Suzuki coupling of 6,6'-dibromo-2,2'-bipyridine and 2-hydroxyphenylboronic acid in DME/H_2O (4:1) medium. The crude obtained after workup was purified in silica column with 20% EtOAc in hexane solution. The corresponding metal complexes were prepared via reaction of the ligand with $Ru(DMSO)_4Cl_2$ and respective ancillary ligands in EtOH in a one-pot synthesis. The complex MCS-B4M was eluted with 1% MeOH in DCM whereas MCS-B5M was eluted with 10% MeOH in DCM from a silica gel column. The synthetic procedure has been outlined in scheme 1.

The complexes MCS-B4M and MCS-B5M sufficiently sensitizes the TiO_2 as observed from the UV-VIS absorption spectra of the metal complexes in solution and composites B4TP and B5TP where all the spectral features of the photosensitizers are well retained in the complex-TiO_2 composites. The attachment of the complex with the TiO_2 surface is stronger in case of B5TP via the -COOH linker groups of isonicotinic acid ligand moieties. In the FTIR spectrum of dye adsorbed TiO_2-Pt composites, there is an overall shift of the peaks towards lower frequencies, thus showing adsorption of the complexes on TiO_2 surface.[25] In B5TP, the carboxylate symmetric and asymmetric peaks are located at 1420 and 1597 cm^{-1}, 177 cm^{-1} apart, whereas in the free complex, they appear at 1382 and 1644 cm^{-1}, the difference being 262 cm^{-1}. This is consistent with the bidentate coordination of the carboxylate groups with TiO_2.

EPR Study

The EPR spectrum of $[Ru(III)(L)(4\text{-picoline})_2]Cl$ (MCS-B4M) is rhombic in nature ($g_x \neq g_y \neq g_z$) (Figure 2).The g values have been assigned as $g_1 = 2.184$, $g_2 = 1.958$ and $g_3 = 1.901$ with the order $g_1 > g_2 > g_3$. From eqn.1, as the $\langle g \rangle$ value of 2.018 is in between the $\langle g \rangle = 2.0023$ corresponding to free electron and $\langle g \rangle > 2.1$ for complete metal based EPR , we can therefore conclude that the EPR signal originates from mixed contributions of both

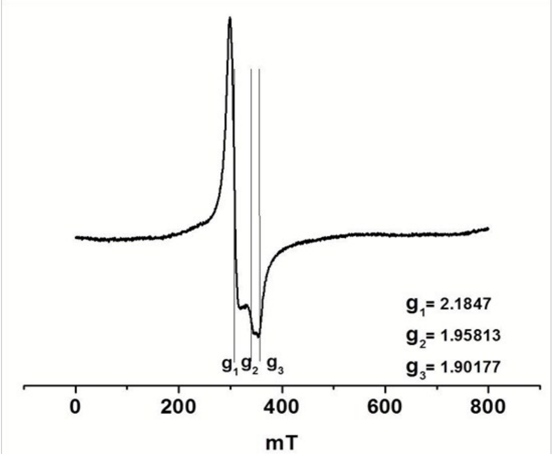

Fig. 2 EPR spectrum of MCS-B4M

metal and ligand.[26]

View Article Online
DOI: 10.1039/C9DT01506J

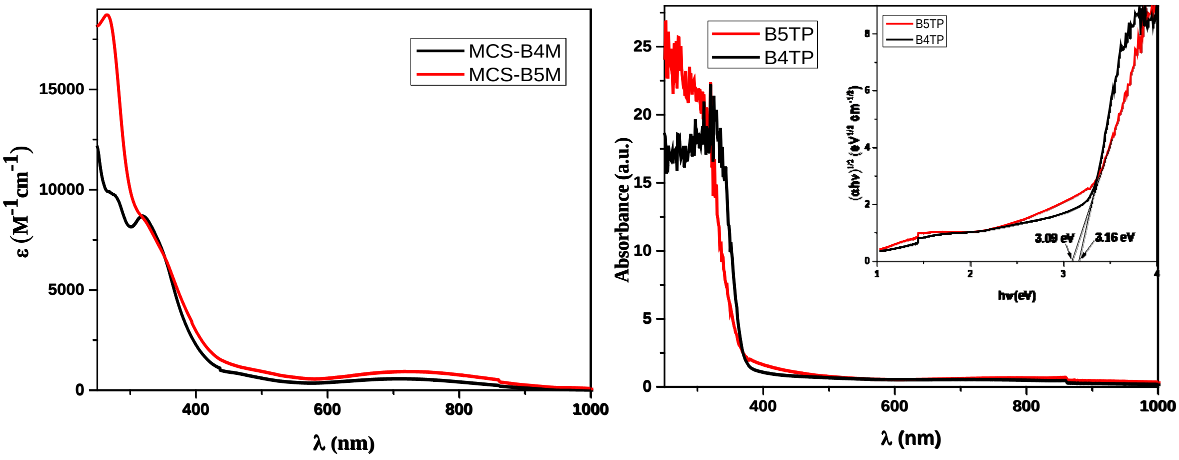

Fig.3. UV-Vis absorption spectra of the complexes in acetonitrile. ***(Left)*** UV-Vis absorption spectra in DRS mode for composites B4TP and B5TP. Inset Tauc Plot of the B4TP and B5TP. ***(right)***

$[\langle g \rangle = {}^{261/2} = 2.018]$ ….(1)
$[\mathrm{As}\ \langle g \rangle = \{(1/3)(g_1^2 + g_2^2 + g_3^2)\}^{1/2}]$

Absorption studies

The synthesized complexes appear green in colour showing a broad absorbance (Figure 3) across the UV-VIS region that may be assigned to a combined effect of ligand based transitions, ligand to metal charge transfer (LMCT) from the phenoxide ligand to the ruthenium centre and metal-ligand to ligand charge transfer (MLL'CT) from ruthenium-phenolate to bipyridine and isonicotinic acid moieties. A prominent less intense peak around 700 nm is also observed accounting for the d-d transitions[26] as inferred from DFT studies (Figure 7 inset). The reflectance mode UV-VIS measurements (DRS) of the complexes/TiO_2-Pt composites replicate the spectral features of the metal complexes in solution. Hence, the TiO_2-Pt composites are properly sensitized with the metal complexes. In both the solution mode as well as DRS mode, the light harvesting capabilities of MCS-B5M is higher than that of MCS-B4M. This is the manifestation of the electron withdrawing nature of the isonicotinic acids resulting in a large transition dipole moment towards the semiconductor interface.[27,28] The band gap values of the composites B5TP and B4TP as calculated from the Tauc plot using Klubeka-Munk formalism are 3.09 eV and 3.16 eV respectively. The lowering of band gap in case of B5TP reflects a better grafting of the MCS-B5M with TiO_2 via the –COOH anchoring groups.[29]

Electrochemical study

The electrochemical properties of both the complexes were studied by means of cyclic voltammetry in acetonitrile (Figure 4). MCS-B4M showed the first anodic peak at 0.78 V corresponding to $Ru^{III/II}$ couple and the oxidation of phenolate moiety to a phenoxyl radical. The second oxidation peak appeared at 1.11 V signifying the Ru(III)-Ru(IV) oxidation whereas in case of MCS-B5M, the anodic peaks for $Ru^{III/II}$ couple appeared at 1.02 V for and Ru(III)-Ru(IV) oxidation at 1.21 V. The higher anodic potential of MCS-B5M as compared to MCS-B4M is presumably due to the electron withdrawing effect of the isonicotinic acid groups[30]. On the cathodic side, the complexes MCS-B4M and MCS-B5M shows a clear reduction around -0.97 V and -0.96V respectively which may be based on the bipyridine moiety as inferred from DFT analysis. The second cathodic peak for MCS-B5M at -1.55 V shows the isonicotinic acid based reductions[31].

Emission studies

The efficiency of electron injection from the excited state of the ruthenium complexes to the conduction band of TiO_2 was examined by means of emission spectroscopy (Figure 5). Although the complexes show high absorption in the UV region, for the purpose of studying the excited state properties on visible light irradiation, both the complexes MCS-B4M and MCS-B5M are excited with light of wavelength 500 nm and 460 nm respectively. In both the cases, the emission was observed at around 550 nm. The emission was rapidly quenched on addition of a miniscule amount of TiO_2-Pt mixture reflecting clear contribution of the metal complex excited states in electron injection.[8] The excited state lifetime decay signal of MCS-B4M and MCS-B5M in acetonitrile solution has been recorded (see Figure S7 in ESI). MCS-B4M records an average lifetime of 1.4 ns fitted with a single exponential decay whereas MCS-B5M registers an average lifetime of 4.9 ns fitted with a multiexponential decay. The higher excited state

View Article Online
DOI: 10.1039/C9DT01506J

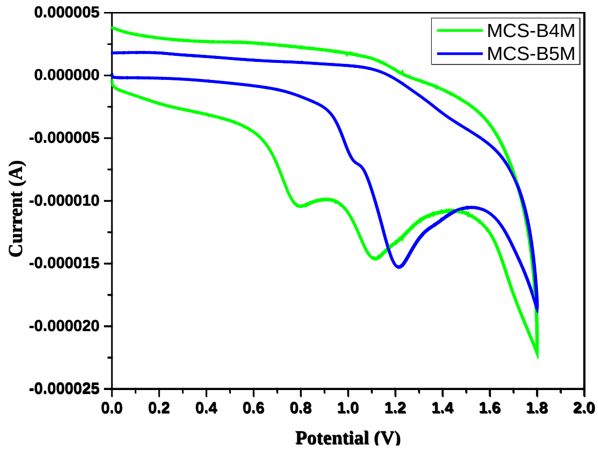

Fig.4. Cyclic Voltammogram of the complexes: anodic wave *(left)* and cathodic wave *(right).*

lifetime for MCS-B5M may be due to the greater delocalization of the metal-centred electron density over the isonicotinic moiety as corroborated later in DFT studies.[32] There was no emission when the complexes were excited at 700 nm.

Photocatalytic hydrogen evolution

The Dye/TiO_2-Pt photocatalysts B4TP and B5TP were tested for photocatalytic performances in aqueous solution with a 300 W xenon lamp and triethanolamine (TEOA) as sacrificial electron donor. The data is summarized in Table 1. For comparison experiments, dye-TiO_2-Pt composite materials were prepared using commercial N719 via the same experimental procedure (Figure 6a and b). It is noteworthy to mention that the performance of MCS-B5M/TiO_2-Pt photocatalyst (TON ~84,600 after 5 h at 0.5 µmol/10 mg catalyst in 2 mL aqueous TEOA solution: pH-7, details in ESI Table S1) surpassed the efficiency of the recent report[18] using more tediously prepared Pt based rhodamine sensitizer (TON 70700 after 40 hours at 0.025 µmol/20 mg catalyst in 5 mL of 1.0 M ascorbic acid solution: pH 4).

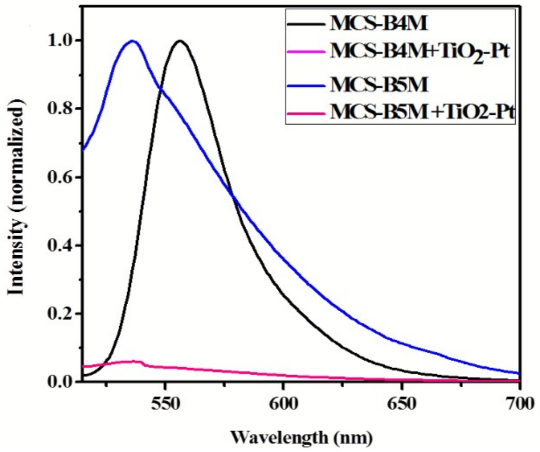

Fig. 5. Emission quenching of the complexes by TiO_2-Pt composite.

Mechanistic aspects for H_2 evolution

From photophysical and electrochemical studies, the two pathways that drive the entire photochemical reactions can be depicted as:

$[Ru^{3+}] + h\nu \rightarrow [^*Ru^{3+}]$……………………………………………………………1

$[^*Ru^{3+}] + TiO_2\text{-Pt} \rightarrow [Ru^{4+}] + TiO_2\text{-Pt}^-$…………………………………….2

$[^*Ru^{3+}] + TEOA \rightarrow [Ru^{2+}] + TEOA_{OX}$……………………………………..3

The oxidative quenching of the complexes with TiO_2-Pt (reaction 2) and subsequent regeneration of the dyes via reductive quenching by TEOA (reaction 3) is energetically feasible[12] as shown:

1. **In the case of B4TP photocatalyst**

The oxidative quenching represented by reaction numbered **4** and the reductive quenching by reaction numbered **5** might be possible quenching mechanisms of $[^*Ru^{3+}]$ by electron transfer:

$[^*Ru^{3+}] + TiO_2\text{-Pt} \rightarrow [[Ru^{4+}] + TiO_2\text{-Pt}^-$ ……4

$TEOA + [^*Ru^{3+}] \rightarrow TEOA_{ox} + [Ru^{2+}]$ …..5

The driving force for the oxidative quenching, reaction **4**, is $\boldsymbol{\Delta G_4}$

$\Delta G_4 = e\,E[Ru^{4+/3+}] - E_{00} - e\,E(TiO_2\text{-Pt}^{0/-})$

$= +1.11\ eV - 3.16\ eV - (-0.6\ eV) = -1.45\ eV.$

The driving force for the reductive quenching, reaction **5**, $\boldsymbol{\Delta G_5}$, is:

$\Delta G_5 = -e\,E(Ru^{3+/2+}) - E_{00} + e\,E([TEOA_{ox}/TEOA)$

$= -(-0.97\ eV) - 3.16eV + 0.82\ eV = -1.37\ eV$

2. **In the case of B5TP photocatalyst**

The oxidative quenching represented by reaction numbered **6** and the reductive quenching by reaction numbered **7** might be possible quenching mechanisms of $[^*Ru^{3+}]$ by electron transfer:

$[^*Ru^{3+}] + TiO_2\text{-Pt} \rightarrow [[Ru^{4+}] + TiO_2\text{-Pt}^-$ …….6

$TEOA + [^*Ru^{3+}] \rightarrow TEOA_{ox} + [Ru^{2+}]$ …….7

The driving force for the oxidative quenching, reaction **6**, is $\boldsymbol{\Delta G_6}$

$\Delta G_6 = e\,E[Ru^{4+/3+}] - E_{00} - e\,E(TiO_2\text{-Pt}^{0/-})$

$= +1.21\ eV - 3.09\ eV - (-0.6\ eV) = -1.28\ eV.$

View Article Online
DOI: 10.1039/C9DT01506J

The driving force for the reductive quenching, reaction **7**, **ΔG_7**, is:

$\Delta G_7 = -e\,E(\mathrm{Ru}^{3+/2+}) - E_{00} + e\,E([\mathrm{TEOA_{ox}}/\mathrm{TEOA})$
$= -(-0.96\ \mathrm{eV}) - 3.09\mathrm{eV} + 0.82\ \mathrm{eV} = -1.31\ \mathrm{eV}$

Therefore, for both the complexes, oxidative and reductive quenching is feasible. DFT studies[22,23] indicate that the HOMO is majorly based on the phenolate moieties and LUMO on the bipyridine moieties of the chelating ligand for both the complexes (Figure 7 inset). Interestingly, for complex MCS-B4M, the HOMO has considerable contribution from the picoline moiety whereas for MCS-B5M, the LUMO is extended to the isonicotinic acid moieties. The significant tuning of the photophysical and electrochemical properties of the metal complexes is achieved by using ancillary ligands with electron donating (4-picoline in MCS-B4M) and electron withdrawing (isonicotinic acid in MCS-B5M) groups. It is apparent that employing our photocatalysts, we achieved higher TON with comparatively lower catalyst loading and shorter irradiation times. The photocatalytic performance of the metal complexes was observed to show two distinct features. Firstly, both the metal complexes (MCS-B4M and MCS-B5M) showed significantly higher H_2 evolution than the standard N719 dye sensitized TiO_2-Pt composites in a similar experimental setup. Similar performance with N719 dye has been reported by others.[24] We attribute the observations to the high oxidation potential of 1.21 V for MCS-B5M as compared to 1.12 V for N719 vs. NHE[33] that results in a faster regeneration of the oxidised complexes[34] by sacrificial electron donor (TEOA in this case). It is worth noting that the apparent quantum efficiency of the B5TP photocatalyst showed impressively high, ~57% at $\lambda \geq 420$ nm (details in ESI). Another interesting feature, the remarkable enhancement in the photocatalytic performance of MCS-B5M/TiO_2-Pt composite as compared to that of MCS-B4M/TiO_2-Pt is presumably due to the better light harvesting capability and higher excited state lifetime coupled with the favourable electronic directionality[35] arising from the proximity of the electron acceptor states to the metal complex-semiconductor interface in the former case. Here, Figure 7 shows an energy diagram representative of the photocatalytic reaction.

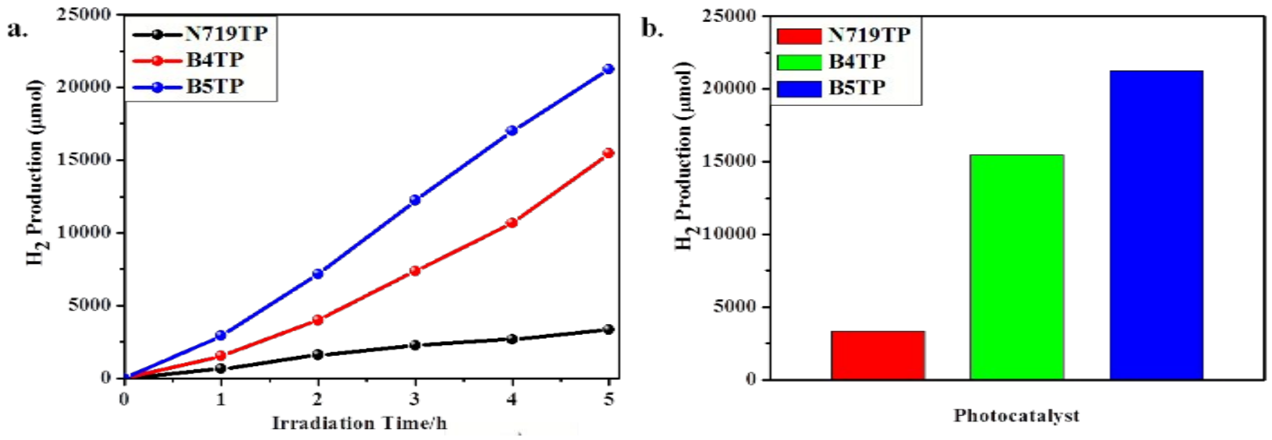

Fig.6 a. Time course of Photocatalytic activities and **b.** Histogram of the MCS-B4M, MCS-B5M and N719 sensitized TiO_2-Pt (B4TP, B5TP and N719TP) in visible-light-driven water splitting; reaction conditions: 0.5 µmol/10 mg catalyst in 20 mL 10 vol% aqueous TEOA solution at pH-7.

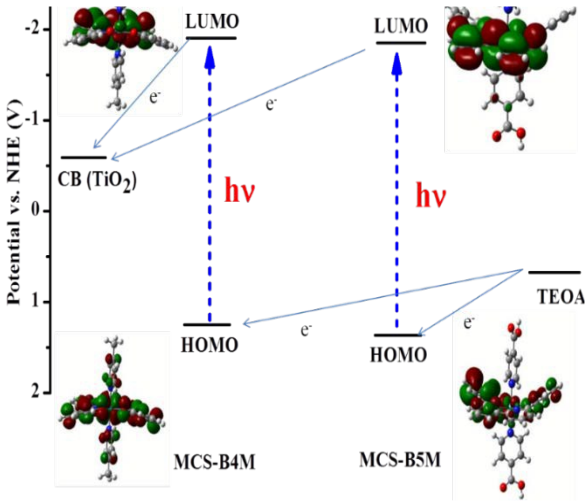

Fig.7 Energy diagram depicting the photocatalytic process of the hybrid systems. The HOMO energy level is determined from the CV of the complexes in aqueous medium. LUMO energy calculated from the relation $E_{LUMO}=E_{HOMO}-E_{00}$.

Table 1. Photocatalytic performance of complexes

Photocatalysts	[a]H_2Production(µmol)	[b]TON	[c]TOF(h^{-1})
B4TP	15467	~61,482	12296
B5TP	21239	~84,600	16920
N719TP	5336	~21,152	4230

[a]H_2 production after 5h. [b]TON (turnover number) = (2 X amount of produced H_2)/amount of catalyst used. [c]TOF (turnover frequency) values after 5h. Reaction conditions: 10 mg photocatalyst (0.5 µmol dye) in 20 mL of 10 vol% neutral aqueous TEOA solution.

Conclusion

In conclusion, two ruthenium-based complexes of bis-(phenolato)bipyridine have been synthesized and studied as

View Article Online
DOI: 10.1039/C9DT01506J

photosensitizers for photocatalytic hydrogen evolution. Among the two complexes, MCS-B5M with –COOH linker moieties at the ancillary ligands exhibit efficient capability of hydrogen evolution of 4.2 $mmolh^{-1}$ and high TON 84,959 after 5 h in the presence of sacrificial electron donor under visible light irradiation. The efficient photochemical performance of the composite is in conformity with the panchromatic light harvesting capability of MCS-B5M throughout the visible light range and a high oxidation potential (E_{ox}=1.21 V for $Ru^{III/IV}$) in aqueous media allowing facile regeneration of the oxidised sensitizer. To the best of our knowledge, this study is the first report of such ruthenium-phenolate complexes working as photosensitizers for visible-light-driven hydrogen evolution from water. Moreover, this work also highlights the importance of ancillary ligands for such photosensitizers in developing effective photocatalyst systems.

Acknowledgements

B.N.M. acknowledges SERB-DST for National Post-Doctoral Fellowship (Ref. No. PDF/2017/001198). A.T. express thanks to CSIR for a Senior Research Fellowship and AcSIR for the Ph.D. enrolment. U.P. and M.C. thanks to DAE/BRNS (GAP-0728) and DST (File No. DST/TM/SERI/FR/92(G) for their respective research grants.

References

1. J. L. L.R. Brown, J.M. Roney, E.E. Adams, *The Great Transition: Shifting from Fossil Fuels to Solar and Wind Energy*, W.W. Norton & Company, New York, First edition edn., 2015.
2. A. J. Bard and M. A. Fox, *Accounts of Chemical Research*, 1995, **28**, 141-145.
3. P. D. Frischmann, K. Mahata and F. Würthner, *Chemical Society Reviews*, 2013, **42**, 1847-1870.
4. L. Cao, D. Chen, W.-Q. Wu, J. Z. Tan and R. A. Caruso, *Journal of Materials Chemistry A*, 2017, **5**, 3645-3654.
5. J. Kiwi and M. Grätzel, *Nature*, 1979, **281**, 657.
6. M. A. Gross, A. Reynal, J. R. Durrant and E. Reisner, *Journal of the American Chemical Society*, 2013, **136**, 356-366.
7. W. J. Youngblood, S.-H. A. Lee, Y. Kobayashi, E. A. Hernandez-Pagan, P. G. Hoertz, T. A. Moore, A. L. Moore, D. Gust and T. E. Mallouk, *Journal of the American Chemical Society*, 2009, **131**, 926-927.
8. K. Maeda, G. Sahara, M. Eguchi and O. Ishitani, *ACS Catalysis*, 2015, **5**, 1700-1707.
9. P. Du, J. Schneider, F. Li, W. Zhao, U. Patel, F. N. Castellano and R. Eisenberg, *Journal of the American Chemical Society*, 2008, **130**, 5056-5058.
10. E. A. Geary, L. J. Yellowlees, L. A. Jack, I. D. Oswald, S. Parsons, N. Hirata, J. R. Durrant and N. Robertson, *Inorganic chemistry*, 2005, **44**, 242-250.
11. C. d. Lentz, O. Schott, T. Auvray, G. Hanan and B. Elias, *Inorganic chemistry*, 2017, **56**, 10875-10881.
12. S. Jasimuddin, T. Yamada, K. Fukuju, J. Otsuki and K. Sakai, *Chemical communications*, 2010, **46**, 8466-8468.
13. R. Abe, K. Shinmei, K. Hara and B. Ohtani, *Chemical Communications*, 2009, 3577-3579.
14. Q. Li, Y. Che, H. Ji, C. Chen, H. Zhu, W. Ma and J. Zhao, *Physical Chemistry Chemical Physics*, 2014, **16**, 6550-6554.
15. A. Tiwari and U. Pal, *international journal of hydrogen energy*, 2015, **40**, e9079.
16. A. Kumari, I. Mondal and U. Pal, *New Journal of Chemistry*, 2015, **39**, 713-720.
17. K. Maeda, M. Eguchi, W. J. Youngblood and T. E. Mallouk, *Chemistry of Materials*, 2009, **21**, 3611-3617.
18. G. Li, M. F. Mark, H. Lv, D. W. McCamant and R. Eisenberg, *Journal of the American Chemical Society*, 2018, **140**, 2575-2586.
19. G. Koyyada, N. S. Pilli, J. H. Jung, K. K. Mandari, B. Shanigaram and M. Chandrasekharam, *International Journal of Hydrogen Energy*, 2018, **43**, 6963-6976.
20. Y. Liu, G. Chen, S. M. Yiu, C. Y. Wong and T. C. Lau, *ChemCatChem*, 2018, **10**, 501-504.
21. D. T. Sawyer, A. Sobkowiak and J. L. Roberts Jr., *Electrochemistry for Chemists*, John Wiley & Sons, New York, second ed. edn., 1995.
22. M. J. Frisch, G. W. Trucks, H. B. Schlegel, G. E. Scuseria, M. A. Robb, J. R. Cheeseman, G. Scalmani, V. Barone, B. Mennucci, G. A. Petersson, H. Nakatsuji, M. Caricato, X. Li, H. P. Hratchian, A. F. Izmaylov, J. Bloino, G. Zheng, J. L. Sonnenberg, M. Hada, M. Ehara, K. Toyota, R. Fukuda, J. Hasegawa, M. Ishida, T. Nakajima, Y. Honda, O. Kitao, H. Nakai, T. Vreven, J. A. Montgomery Jr., J. E. Peralta, F. Ogliaro, M. J. Bearpark, J. Heyd, E. N. Brothers, K. N. Kudin, V. N. Staroverov, R. Kobayashi, J. Normand, K. Raghavachari, A. P. Rendell, J. C. Burant, S. S. Iyengar, J. Tomasi, M. Cossi, N. Rega, N. J. Millam, M. Klene, J. E. Knox, J. B. Cross, V. Bakken, C. Adamo, J. Jaramillo, R. Gomperts, R. E. Stratmann, O. Yazyev, A. J. Austin, R. Cammi, C. Pomelli, J. W. Ochterski, R. L. Martin, K. Morokuma, V. G. Zakrzewski, G. A. Voth, P. Salvador, J. J. Dannenberg, S. Dapprich, A. D. Daniels, Ö. Farkas, J. B. Foresman, J. V. Ortiz, J. Cioslowski and D. J. Fox, *Journal*, 2009.
23. F. Weigend and R. Ahlrichs, *Physical Chemistry Chemical Physics*, 2005, **7**, 3297-3305.
24. J. Lee, J. Kwak, K. C. Ko, J. H. Park, J. H. Ko, N. Park, E. Kim, T. K. Ahn, J. Y. Lee and S. U. Son, *Chemical Communications*, 2012, **48**, 11431-11433.
25. C. Pérez León, L. Kador, B. Peng and M. Thelakkat, *The Journal of Physical Chemistry B*, 2006, **110**, 8723-8730.
26. H. Arora, C. Philouze, O. Jarjayes and F. Thomas, *Dalton Transactions*, 2010, **39**, 10088-10098.
27. T. W. Rees and E. Baranoff, *Polyhedron*, 2014, **82**, 37-49.
28. H.-J. Park, K. H. Kim, S. Y. Choi, H.-M. Kim, W. I. Lee, Y. K. Kang and Y. K. Chung, *Inorganic chemistry*, 2010, **49**, 7340-7352.
29. O. Suryani, Y. Higashino, J. Y. Mulyana, M. Kaneko, T. Hoshi, K. Shigaki and Y. Kubo, *Chemical Communications*, 2017, **53**, 6784-6787.
30. A. K. Pal, S. Nag, J. G. Ferreira, V. Brochery, G. La Ganga, A. Santoro, S. Serroni, S. Campagna and G. S. Hanan, *Inorganic chemistry*, 2014, **53**, 1679-1689.
31. S. H. Wadman, J. M. Kroon, K. Bakker, R. W. Havenith, G. P. van Klink and G. van Koten, *Organometallics*, 2010, **29**, 1569-1579.

View Article Online
DOI: 10.1039/C9DT01506J

32. E. A. Medlycott and G. S. Hanan, *Chemical Society Reviews*, 2005, **34**, 133-142.
33. G. Boschloo and A. Hagfeldt, *Accounts of chemical research*, 2009, **42**, 1819-1826.
34. Y. Liu, S.-X. Guo, A. M. Bond, J. Zhang, Y. V. Geletii and C. L. Hill, *Inorganic chemistry*, 2013, **52**, 11986-11996.
35. I. Mondal, A. Tiwari, R. Ghosh and U. Pal, *RSC Advances*, 2016, **6**, 41165-41172.